

# Skimming, Locating, then Perusing: A Human-Like Framework for Natural Language Video Localization

Daizong Liu  
dzliu@stu.pku.edu.cn  
Wangxuan Institute of Computer  
Technology, Peking University  
Beijing, China

Wei Hu<sup>†</sup>  
forhuwei@pku.edu.cn  
Wangxuan Institute of Computer  
Technology, Peking University  
Beijing, China

## ABSTRACT

This paper addresses the problem of natural language video localization (NLVL). Almost all existing works follow the “only look once” framework that exploits a single model to directly capture the complex cross- and self-modal relations among video-query pairs and retrieve the relevant segment. However, we argue that these methods have overlooked two indispensable characteristics of an ideal localization method: 1) Frame-differentiable: considering the imbalance of positive/negative video frames, it is effective to highlight positive frames and weaken negative ones during the localization. 2) Boundary-precise: to predict the exact segment boundary, the model should capture more fine-grained differences between consecutive frames since their variations are often smooth. To this end, inspired by how humans perceive and localize a segment, we propose a two-step human-like framework called Skimming-Locating-Perusing (SLP). SLP consists of a Skimming-and-Locating (SL) module and a Bi-directional Perusing (BP) module. The SL module first refers to the query semantic and selects the best matched frame from the video while filtering out irrelevant frames. Then, the BP module constructs an initial segment based on this frame, and dynamically updates it by exploring its adjacent frames until no frame shares the same activity semantic. Experimental results on three challenging benchmarks show that our SLP is superior to the state-of-the-art methods and localizes more precise segment boundaries.

## CCS CONCEPTS

• Information systems → Video search; Novelty in information retrieval.

## KEYWORDS

Natural language video localization, Skimming-and-locating, Bi-directional perusing, Human-like

## ACM Reference Format:

Daizong Liu and Wei Hu<sup>†</sup>. 2022. Skimming, Locating, then Perusing: A Human-Like Framework for Natural Language Video Localization. In *Proceedings of the 30th ACM International Conference on Multimedia (MM '22)*, October 10–14, 2022, Lisboa, Portugal.

Permission to make digital or hard copies of all or part of this work for personal or classroom use is granted without fee provided that copies are not made or distributed for profit or commercial advantage and that copies bear this notice and the full citation on the first page. Copyrights for components of this work owned by others than ACM must be honored. Abstracting with credit is permitted. To copy otherwise, or republish, to post on servers or to redistribute to lists, requires prior specific permission and/or a fee. Request permissions from [permissions@acm.org](mailto:permissions@acm.org).

MM '22, October 10–14, 2022, Lisboa, Portugal

© 2022 Association for Computing Machinery.

ACM ISBN 978-1-4503-9203-7/22/10...\$15.00

<https://doi.org/10.1145/3503161.3547782>

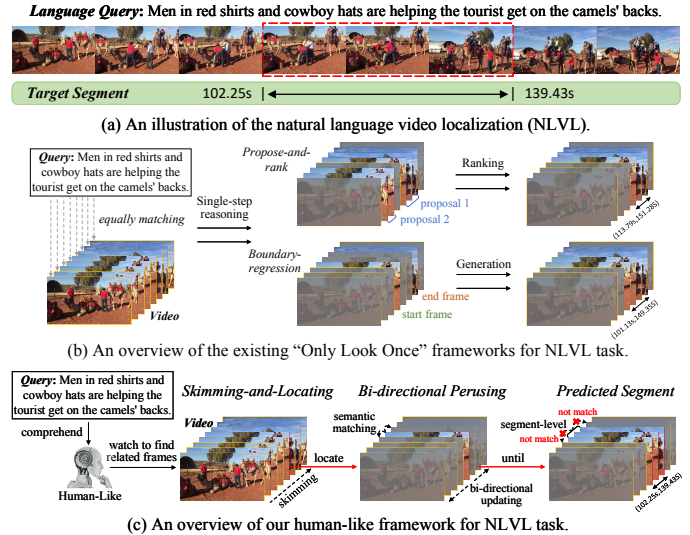


Figure 1: (a) An illustrative example of the NLVL task. (b) The overview of the existing “only look once” frameworks, which equally learn the frame-word and frame-frame relations and predict the segment via a single-step reasoning model. (c) The overview of our human-like framework, which first skims the entire video to locate the most relevant frame according to the query semantic, then peruses its adjacent frames to construct and update more accurate segment.

October 10–14, 2022, Lisboa, Portugal. ACM, New York, NY, USA, 10 pages.  
<https://doi.org/10.1145/3503161.3547782>

## 1 INTRODUCTION

Natural language video localization (NLVL) is an important yet challenging task in multimedia understanding, which has drawn increasing attention in recent years due to its vast potential applications in information retrieval [32, 48] and human-computer interaction [19, 42]. This task aims to localize a specific video segment that semantically corresponds to a sentence query, as shown in Figure 1 (a). NLVL requires not only the modeling of the complex multi-modal interactions among vision and language, but also the characterization of complicated contexts for semantic alignment.

<sup>†</sup>This work is supported by the National Key R&D Program of China under contract No. 2021YFF0901502. Corresponding author: Wei Hu ([forhuwei@pku.edu.cn](mailto:forhuwei@pku.edu.cn)).

Most existing works [1, 12, 51, 59, 60] tackle the NLVL following a *propose-and-rank* architecture, which first predefines multiple segment candidates of different time intervals and then ranks them according to their semantic similarities with the query. The best segment is selected based on the similarities. These methods are sensitive to the quality of segment candidates and are inefficient due to redundant candidate-query matching. Recently, several works [8, 52, 56, 57] exploit a more efficient *boundary-regression* architecture that directly predicts the start/end boundaries of the target segment. However, they neglect the rich internal information between start and end boundaries without capturing the segment-level interaction. Whether adopting *propose-and-rank* or *boundary-regression* architecture, almost all current methods follow the “only look once” strategy that equally learns the relations between all frame-word and frame-frame pairs of the matched video-query within a single modeling process. The segment is subsequently predicted based on all query-guided frame features. Details are shown in Figure 1 (b).

In this paper, we argue that these methods are unnatural to human perceptions and have overlooked two indispensable characteristics of an ideal localization strategy: 1) Frame-differentiable: A video often contains thousands of frames, but maybe only a few positive frames are related to the query. Instead of predicting the segments by equally considering all frames, it is more effective to highlight positive frames and weaken negative ones during the localization. 2) Boundary-precise: It is challenging to distinguish visually similar contents in consecutive frames of a video with the “only look once” strategy, since the variation between the adjacent frames is often smooth. Instead of relying on the single-step reasoning, it is required to deeply mine more fine-grained differences between adjacent frames for precisely locating the segment boundaries. Luckily, the above two characteristics have already been captured by human brain and are the key reasons why humans are able to retrieve the exact segment effectively. As shown in Figure 1 (c), given a video-query pair, humans generally first comprehend the query semantic and skim through the video to locate the most matched frame. Based on this matched frame, humans then gradually peruse and decide whether its adjacent frames share the same semantic related to the target activity. The predicted segment is determined when no adjacent frames match the activity semantic. Such human-aware localization strategy can also alleviate the problems of redundant candidates and lacking internal information in *propose-and-rank* and *boundary-regression* frameworks.

To this end, inspired by how humans localize a segment in a video, we propose a human-like framework for NLVL—Skimming-Locating-Perusing (SLP), which develops a “two-step” localization strategy to determine accurate segment boundaries. We first develop a Skimming-and-Locating (SL) module to imitate human perceptions that locate the most likely positive frames corresponding to query semantic by skimming through the entire video. In SL module, we comprehend the aligned semantics between the video-query pair and highlight the relevant frames as well as suppress irrelevant ones for discriminative frame-wise representation learning, which is realized by a query-guided content comprehension network. Then, we propose a Bi-directional Perusing (BP) module to dynamically construct segments based on the previously predicted positive frames. Specifically, the BP module takes each predicted positive frame as the initial segment, and then gradually adds the

adjacent frames into the segment if they share the same linguistic query or visual appearance semantic. This perusing strategy exploits fine-grained differences among consecutive frames, leading to more precise segment boundary localization.

Our main contributions are summarized as follows:

- Firstly, we propose a novel Skimming-Locating-Perusing (SLP), which is the first human-like framework for NLVL to take both frame-differentiable and boundary-precise requirements into account to the best of our knowledge.
- Secondly, different from the “only look once” localization strategy, our “two-step” SL and BP modules highlight more impact on the positive frames and capture more fine-grained differences between adjacent frames.
- Finally, experiments validate the effectiveness of SLP over three challenging benchmarks ActivityNet Caption, TACoS and Charades-STA.

## 2 RELATED WORKS

**Natural language image retrieval.** Early works of localization task mainly focus on localizing the image region corresponding to a language query. They first generate candidate image regions using image proposal method [37], and then find the matched one with respect to the given query. Some works [15, 31, 39] try to extract target image regions based on description reconstruction error or probabilities. There are also several studies [6, 7, 50, 55] considering incorporating contextual information of region-phrase relationship into the localization model. [45] further models region-region and phrase-phrase structures. Some other methods exploit attention modeling in queries, images, or object proposals [10, 11, 49].

**Natural language video localization.** Natural language video localization (NLVL) is a new task introduced recently [1, 12]. Various algorithms [1, 5, 12, 21–24, 26, 28, 29, 51, 59, 60] have been proposed within the *propose-and-rank* framework, which first generates segment candidates and then utilizes multimodal matching to retrieve the most relevant candidate for a query. Some of them [1, 12] take multiple sliding windows as candidates. To improve the quality of the candidates, [51, 60] pre-cut the video on each frame by multiple pre-defined temporal scales, and directly integrate sentence information with fine-grained video clip for scoring. For instance, Xu *et al.* [47] introduce a multi-level model to integrate visual and textual features earlier and further re-generate queries as an auxiliary task. Chen *et al.* [5] capture the evolving fine-grained frame-by-word interactions between video and query to enhance the video representation understanding. Zhang *et al.* [54] model relations among candidate segments produced from a convolutional neural network with the guidance of the query information. Although these methods achieve great performance, they are severely limited by the heavy computation on proposal matching/ranking, and sensitive to the quality of pre-defined proposals.

Recently, many methods [8, 25, 27, 33, 34, 38, 52, 53, 56, 57] propose to utilize the *boundary-regression* framework. Specifically, instead of relying on the segment candidates, they directly predict two probabilities at each frame by leveraging cross-modal interactions between video and query, which indicate whether this frame is a start/end frame of the ground truth video segment. There are

also some reinforcement learning (RL) based frameworks [14, 46] proposed in the NLVL task.

However, almost all the above two classes of methods equally learn the complex frame-to-word and frame-to-frame relations within a single modeling process and retrieve the segment based on all frames, which often fails to distinguish the foreground-background frames and capture the fine-grained differences between certain consecutive frames for determining precise segment boundaries.

### 3 METHODOLOGY

#### 3.1 Problem Statement

Given an untrimmed video  $\mathcal{V}$ , we represent it as  $\mathcal{V} = \{v_t\}_{t=1}^T$  frame-by-frame, where  $v_t$  is the  $t$ -th frame and  $T$  is the length of the entire video. We denote the given sentence query with  $N$  words as  $Q = \{q_n\}_{n=1}^N$  word-by-word, where  $q_n$  is the  $n$ -th word in the query. The NLVL task aims to localize a segment in video  $\mathcal{V}$  starting at timestamp  $\tau_s$  and ending at timestamp  $\tau_e$ , which corresponds to the query  $Q$  semantically. This task is quite challenging since it is difficult to localize activities of interest precisely in a long video with complex contents.

#### 3.2 Overview

We focus on addressing the issue that existing NLVL methods with the “only look once” strategy are unnatural to human perceptions and often fail to mine more fine-grained differences between adjacent frames for precise boundary prediction. To this end, we propose a human-like framework to imitate how humans localize the segment associated to the query. Instead of following the “only look once” strategy to utilize a single-step reasoning process, we introduce a novel two-step localization paradigm of “Skimming-Locating-Perusing” (SLP), which consists of two main modules as shown in Figure 2: (1) **Skimming-and-Locating (SL) module**: It first predicts the most query-related positive frames by fine-grained multi-modal reasoning for filtering out negative ones; (2) **Bi-directional Perusing (BP) module**: After obtaining the positive frames, it then dynamically constructs desired segment by finely searching and adding semantically similar adjacent frames based on each predicted positive frame. In such a coarse-to-fine manner, we are able to determine more precise segment boundaries.

Formally, we first forward the input video  $\mathcal{V} = \{v_t\}_{t=1}^T$  and the query  $Q = \{q_n\}_{n=1}^N$  to the SL module for multi-modal feature encoding and interaction. Then it selects the foremost matched frames related to the query as the positive frames by:

$$\{y_t\}_{t=1}^T = \text{SL}(\mathcal{V}, Q), \quad (1)$$

where  $y_t \in \{0, 1\}$  is a binary class to determine whether the  $t$ -th frame is positive or negative.

With the predicted frame-wise class  $\{y_t\}_{t=1}^T$ , the BP module constructs the desired segment based on each predicted positive frame by bi-directionally searching its adjacent frames sharing the same activity semantically. In particular, it first takes one of the predicted positive frames as the initial segment and then dynamically updates

this segment by:

$$\begin{aligned} (t-1, t+1) &= \text{BP}((t, t), \mathcal{V}, Q), \\ &\dots \\ (t-l_s, t+l_e) &= \text{BP}((t-l_s, t+l_e-1), \mathcal{V}, Q), \end{aligned} \quad (2)$$

where  $t$  is the index of the selected positive frame and  $(t, t)$  denotes the initial segment. The final predicted segment  $(t-l_s, t+l_e)$  is constructed by iteratively searching the adjacent frames near the segment boundary and updating the segment with the semantically related adjacent frames. Specifically, whether adjacent frames near the boundary are added to the segment depends on whether they share both the same query-guided and visual-related semantics to the segment.

**Inference details.** Given an input video-query pair, we first forward them through the SL module to predict top  $K$  positive frames. Then, for each positive frame, we initialize the corresponding segment and deploy the BP module to dynamically update it. The final localization result is obtained by choosing the segment among the  $K$  constructed ones with the highest confidence score.

In the following, we first elaborate on the SL module and BP module, respectively. Then, we present the training details of the proposed SLP model.

#### 3.3 Skimming-and-Locating Module

**Multi-modal encoders.** Given a video  $\mathcal{V} = \{v_t\}_{t=1}^T$  with  $T$  frames, we first extract its features by a pre-trained C3D network [43], and then employ a multi-head self-attention [44] module to capture the long-range dependencies among the video frames. We also utilize a Bi-GRU [9] layer to learn the sequential characteristic. The final video features are denoted as  $V = \{v_t\}_{t=1}^T \in \mathbb{R}^{T \times D}$ , where  $D$  is the feature dimension. For query  $Q$  encoding, following previous works [53, 60], we first generate the word-level embeddings using the Glove [35] embeddings, and then employ another multi-head self-attention module and Bi-GRU layer to further encode the query features as  $Q = \{q_n\}_{n=1}^N \in \mathbb{R}^{N \times D}$ .

**Query-guided content comprehension.** To skim and locate the most positive frames related to the query semantic, it is natural to learn and enhance the video-query interaction for frame-wise discriminative representation learning. Therefore, we propose a query-guided content comprehension (QCC) submodule which consists of two stages: 1) We first associate frame-wise video features with the correlated word-wise query features to obtain the multi-modal features. 2) Then, we construct a multi-modal graph over the multi-modal features by connecting frame-wise nodes referring the query-guided semantic similarity of neighbors. By reasoning over this graph, the responses of the positive frames matched with the query cue are highlighted while those of non-matched ones are suppressed accordingly. Finally, the enhanced multi-modal features are utilized to predict the positive frames. Comparing with previous works equally learns the frame-wise relations, our QCC module provides more fine-grained frame-wise semantic understanding by query-relevant/irrelevant frame distinguishment for predicting more accurate positive frames.

In the first stage, given the encoded features of video and query  $V, Q$ , we adopt a typical attention mechanism to associate query information with the video features of each frame. Concretely, we first

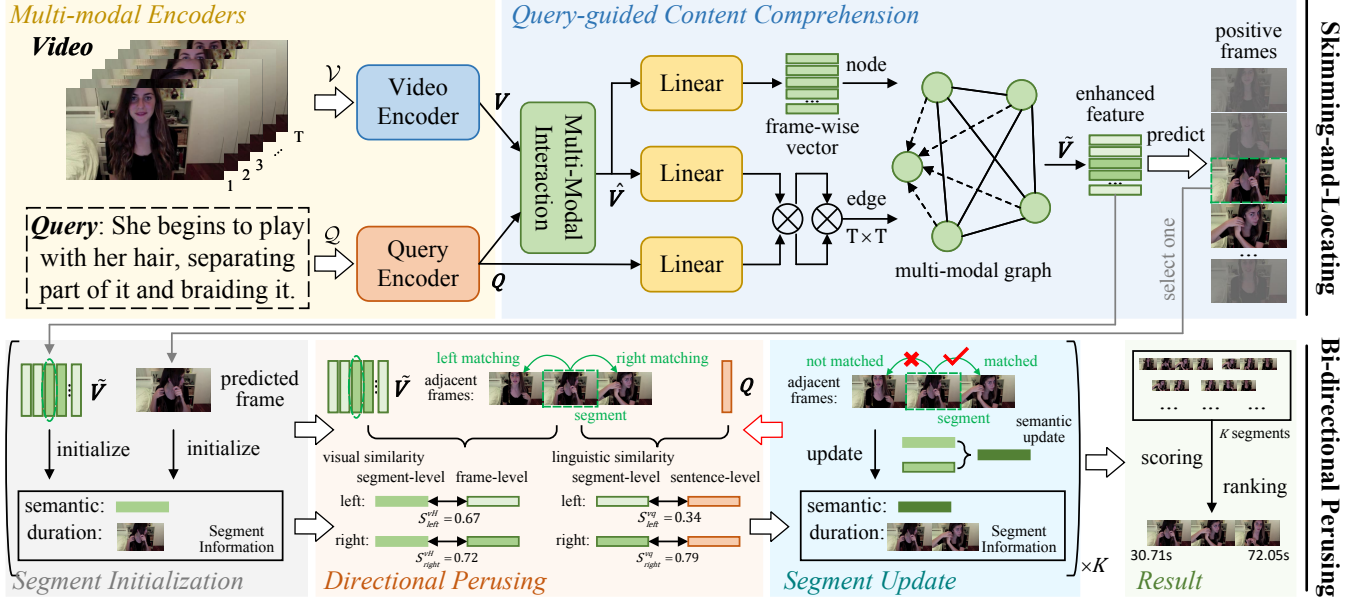


**Figure 2: An overview of the proposed Skimming-Locating-Perusing (SLP) architecture for NLVL. The Skimming-and-Locating (SL) module first predicts the top- $K$  ranked positive frames among the entire video. Then, the Bi-directional Perusing (BP) module dynamically constructs and updates the segment based on each predicted positive frame. The final segment is selected based on the learned confidence score.**

compute the attention score between each pair of frame and word, and obtain a video-to-query attention matrix  $M = \{m_{t,n}\}_{t=1, n=1}^{t=T, n=N} \in \mathbb{R}^{T \times N}$ . Each score  $m_{t,n}$  represents the correlation of the  $t$ -th frame and  $n$ -th word, and is formulated by:

$$m_{t,n} = \mathbf{w}^\top \tanh(\mathbf{W}_1^m \mathbf{v}_t + \mathbf{W}_2^m \mathbf{q}_n + \mathbf{b}^m), \quad (3)$$

where  $\mathbf{W}_1^m, \mathbf{W}_2^m, \mathbf{b}^m$  are learnable parameters, and  $\mathbf{w}^\top$  is a row vector [60]. The query-guided frame features  $\hat{\mathbf{v}}_t$  is obtained by:

$$\hat{\mathbf{v}}_t = [\mathbf{v}_t; \sum_{n=1}^N \text{softmax}(m_{t,n})(\mathbf{W}^Q \mathbf{q}_n)], \quad (4)$$

where  $\mathbf{W}^Q$  projects query contexts into the video domain. By integrating both video and query contexts into the multi-modal features  $\tilde{\mathbf{V}} = \{\hat{\mathbf{v}}_t\}_{t=1}^T \in \mathbb{R}^{T \times 2D}$ , all foreground frames that might be referred to the query semantic are perceived appropriately.

In the second stage, we regard each query-guided frame feature  $\hat{\mathbf{v}}_t$  as a node and construct a fully-connected graph which is composed of  $T$  nodes. In order to selectively highlight the positive frames while weakening the background ones, we define the edge weights depending on affinities between connected frames and query semantic. The adjacency matrix  $\mathbf{A} \in \mathbb{R}^{T \times T}$  is formulated as:

$$\begin{aligned} \mathbf{B} &= (\tilde{\mathbf{V}} \mathbf{W}_1^A) (\tilde{\mathbf{Q}} \mathbf{W}_2^A)^\top, \\ \mathbf{A} &= \text{softmax}(\mathbf{B}) \text{softmax}(\mathbf{B}^\top), \end{aligned} \quad (5)$$

where  $\mathbf{W}_1^A, \mathbf{W}_2^A$  are learnable parameters, and  $\mathbf{B} \in \mathbb{R}^{T \times N}$ . Each element of  $\mathbf{A}$  represents the normalized magnitude of information flow from one frame to another, which depends on their affinities with the query semantic. Therefore, we apply a graph convolution

layer [17] to enhance discriminative representation learning:

$$\tilde{\mathbf{V}} = (\mathbf{A} + \mathbf{I}) \tilde{\mathbf{V}} \mathbf{W}_3^A, \quad (6)$$

where  $\mathbf{I}$  is an identity matrix for adding self-loops.  $\tilde{\mathbf{V}} \in \mathbb{R}^{T \times D}$  is the enhanced features, achieving the “skimming” process analogous to the comprehension of query-guided video contents by humans.

Subsequently, we apply a binary classification function on the obtained multi-modal features  $\tilde{\mathbf{V}}$  to “locate” the most probable positive video frames falling into the ground-truth segment. To this end, we design a binary classification module with three linear layers to predict the class  $y_t$  on each frame  $t$ . Since we capture the fine-grained query-guided frame-to-frame relations in the “skimming” process, the learned multi-modal feature  $\tilde{\mathbf{V}}$  is able to predict the positive frames well (demonstrated by the visualization results in the experiments). We define the binary cross-entropy loss as:

$$\mathcal{L}_{class} = -\frac{1}{T} \sum_{t=1}^T y_t^{gt} \log(y_t) + (1 - y_t^{gt}) \log(1 - y_t), \quad (7)$$

where  $y_t^{gt}$  is the ground truth. The predicted top- $K$  ranked frames are taken as the positive frames.

### 3.4 Bi-directional Perusing

**Segment initialization.** Given one of the top- $K$  ranked frames indexed at time  $t$  predicted by the features  $\tilde{\mathbf{V}}$ , we take it as the initial segment  $(t, t)$  and initialize its feature as  $\mathbf{H}_{t:t} = \tilde{\mathbf{v}}_t \in \mathbb{R}^D$ , where  $t : t$  denotes the segment duration. The semantic feature of the segment  $\mathbf{H}_{t:t}$  will be updated by dynamically adding semantically relevant adjacent frames to it.

**Directional perusing.** Based on the initial segment  $\mathbf{H}_{t:t}$ , there are three human-like ways to dynamically peruse the adjacent

frames of the current segment: 1) perusing the left frames until no frame matches the target semantic before perusing the right ones; 2) perusing the right frames until no frame matches the target semantic before perusing the left ones; 3) perusing the left and right frames at the same time. Here, we take the first perusing way as an example to illustrate our directional perusing process. Analysis of adopting other ways will be shown in our experiments.

Given the current segment  $\mathbf{H}_{t:t}$  and its left adjacent frame  $\tilde{\mathbf{v}}_{t-1}$ , we formulate a matching score  $S(\tilde{\mathbf{v}}_{t-1}, \mathbf{H}_{t:t})$  to determine whether the  $(t-1)$ -th frame should be added into the current segment. We define this matching score  $S(\tilde{\mathbf{v}}_{t-1}, \mathbf{H}_{t:t})$  as:

$$S(\tilde{\mathbf{v}}_{t-1}, \mathbf{H}_{t:t}) = \alpha_1 S_{t-1,t:t}^{vq} + \alpha_2 S_{t-1,t:t}^{vH}, \quad (8)$$

where  $\alpha_1, \alpha_2$  are balancing parameters. The matching score is composed of two terms: 1)  $S_{t-1,t:t}^{vq}$  measures the *linguistic similarity* between the semantics of frame  $\tilde{\mathbf{v}}_{t-1}$  and the query  $\mathbf{Q}$ ; 2)  $S_{t-1,t:t}^{vH}$  measures the *visual similarity* between the semantics of frame  $\tilde{\mathbf{v}}_{t-1}$  and segment  $\mathbf{H}_{t:t}$ . Both two semantic similarities are crucial to distinguish the query-relevant/irrelevant adjacent frames. In particular, we employ cosine similarity to formulate them as:

$$S_{t-1,t:t}^{vq} = \sum_{n=1}^N \cos(\tilde{\mathbf{v}}_{t-1}, \mathbf{q}_n) / N, \quad (9)$$

$$S_{t-1,t:t}^{vH} = \cos(\tilde{\mathbf{v}}_{t-1}, \mathbf{H}_{t:t}).$$

To supervise both above frame-query and frame-segment matching during the training, we adopt a hinge-based triplet ranking loss [16] to encourage the similarity score of matched pairs to be larger than those of mismatched pairs as follows:

$$\begin{aligned} \mathcal{L}_{match}^{vq} &= \max(0, \beta_1 - S^{vq} + S^{\bar{v}q}), \\ &\quad + \max(0, \beta_1 - S^{vq} + S^{v\bar{q}}), \\ \mathcal{L}_{match}^{vH} &= \max(0, \beta_2 - S^{vH} + S^{\bar{v}H}) \\ &\quad + \max(0, \beta_2 - S^{vH} + S^{v\bar{H}}), \\ \mathcal{L}_{match} &= \text{avg}(\sum \gamma_1 \mathcal{L}_{match}^{vq} + \gamma_2 \mathcal{L}_{match}^{vH}), \end{aligned} \quad (10)$$

where  $\beta_1, \beta_2$  and  $\gamma_1, \gamma_2$  are the margin and balancing parameters, respectively.  $S^{vq}$  is the score of the matched frame-query,  $S^{\bar{v}q}, S^{v\bar{q}}$  are the scores of the mismatched frame-query. Analogously,  $S^{vH}$  is the score of the matched frame-segment, while  $S^{\bar{v}H}, S^{v\bar{H}}$  are the mismatched ones. Note that, we define the random negative frame/segment (outside the ground-truth segment) as the mismatched frame or mismatched segment, and denote all segment candidates within the ground-truth segment as the matched segments.  $\text{avg}(\cdot)$  is the average operation.

**Segment update.** Once the above matching score  $S(\tilde{\mathbf{v}}_{t-1}, \mathbf{H}_{t:t})$  is larger than a pre-defined threshold  $\Theta$ , we will add the adjacent frame  $\tilde{\mathbf{v}}_{t-1}$  into the segment, leading to an expanded segment  $\mathbf{H}_{t-1:t} \in \mathbb{R}^D$ . Instead of directly adopting max-pooling to update the segment as in [59], we introduce a new and learnable segment updating strategy to keep the most semantic-related discriminative information and filter out the unimportant one for each new frame since the target activity mostly happens in a local region of the whole frame (the other regions provide redundant information).

Specifically, we first compute the intermediate segment semantic by adding the content of new frame:

$$(\mathbf{H}_{t-1:t})' = \tanh(\mathbf{W}_1^H (\mathbf{r}_1 \odot \tilde{\mathbf{v}}_{t-1}) + \mathbf{U}_1^H (\mathbf{r}_2 \odot \mathbf{H}_{t:t}) + \mathbf{b}_1^H), \quad (11)$$

where  $\mathbf{W}_1^H, \mathbf{U}_1^H$  and  $\mathbf{b}_1^H$  are weights and bias,  $\odot$  is an element-wise multiplication.  $\mathbf{r}_1, \mathbf{r}_2$  are the reset gates learned to forget the background contents in each frame, which are formulated as:

$$\mathbf{r}_i = \text{sigmoid}(\mathbf{W}_i^r \tilde{\mathbf{v}}_{t-1} + \mathbf{U}_i^r \mathbf{H}_{t:t} + \mathbf{b}_i^r), i = 1, 2 \quad (12)$$

where  $\mathbf{W}_i^r, \mathbf{U}_i^r$  and  $\mathbf{b}_i^r$  are weights and bias. To decide how much the intermediate semantic  $(\mathbf{H}_{t-1:t})'$  updates the previous segment  $\mathbf{H}_{t:t}$ , we develop a gate  $\mathbf{z}$  similarly to the reset gate  $\mathbf{r}_i$  and formulate the updating process as:

$$\begin{aligned} \mathbf{z} &= \text{sigmoid}(\mathbf{W}^z \tilde{\mathbf{v}}_{t-1} + \mathbf{U}^z \mathbf{H}_{t:t} + \mathbf{b}^z), \\ \mathbf{H}_{t-1:t} &= \mathbf{z} \odot (\mathbf{H}_{t-1:t})' + (1 - \mathbf{z}) \odot \mathbf{H}_{t:t}, \end{aligned} \quad (13)$$

where  $\mathbf{W}^z, \mathbf{U}^z$  and  $\mathbf{b}^z$  are weights and bias. The updated segment  $\mathbf{H}_{t-1:t}$  focuses on more precise activity-guided semantics related to the query. We iteratively update segment using the BP module until no adjacent frames match the activity semantic.

To supervise the segment updating and indicate the quality of each construct segment, we introduce an IoU regression head based on each segment feature  $\mathbf{H}_{t-1:t}$  to predict its confidence score. Specifically, we train a three-layer linear network and acquire the corresponding confidence score  $c_{t-1:t}$ . The training target  $c_{t-1:t}^{gt}$  is obtained by calculating the IoU between segment  $(t-1, t)$  and the ground-truth segment  $(\tau_s, \tau_e)$ . We define the regression loss function as:

$$\mathcal{L}_{conf} = \text{avg}(\sum \mathcal{R}_1(c_{t-1:t}, c_{t-1:t}^{gt})), \quad (14)$$

where  $\mathcal{R}_1$  is the Smooth-L1 loss [13]. Therefore, we can predict the confidence scores of the final  $K$  constructed segment and choose the best one as the result according to their scores.

### 3.5 Training Details

To ensure both SL and BP modules properly, we develop a three-stage training algorithm for our proposed SLP model. **In stage 1**, since the positive frame localization process (binary classification) in SL module often fails to produce high-quality predictions at the beginning of training, we leave the BP module out of this stage and only train the SL module by minimizing Equation (7) for warming up. **In stage 2**, we first fix the SL module obtained in stage 1, and then only train the BP module. Specifically, we enumerate possible frame-query and frame-segment pairs to minimize Equation (10), and update possible segments initialized from random positive frames for minimizing Equation (14). **In stage 3**, we fine-tune the entire model in an end-to-end manner, which further improves the overall performance of our method.

## 4 EXPERIMENTS

### 4.1 Datasets and Evaluation Metrics

**ActivityNet Caption.** Activity Caption [18] contains 20000 videos with 100000 descriptions from YouTube [2]. The videos are 2 minutes on average, and these annotated video clips have much larger variation, ranging from several seconds to over 3 minutes. Since the test split is withheld for competition, following public split [12],

we use 37421, 17505, and 17031 sentence-video pairs for training, validation, and testing respectively.

**TACoS.** TACoS is collected by [36] for video grounding and dense video captioning tasks. It consists of 127 videos on cooking activities with an average length of 4.79 minutes. In video grounding task, it contains 18818 video-query pairs. For fair comparisons, we follow the same split of the dataset as [12], which has 10146, 4589, and 4083 video-query pairs for training, validation, and testing respectively.

**Charades-STA.** Charades-STA is a benchmark dataset for the video grounding task, which is built upon the Charades [40] dataset. It is collected for video action recognition and video captioning, and contains 6672 videos and involves 16128 video-query pairs. Following previous work [12], we utilize 12408 video-query pairs for training and 3720 pairs for testing.

**Evaluation metric.** We adopt “R@n, IoU=m” proposed by [15] as the evaluation metric, which calculates the IoU between the top-n retrieved video segments and the ground truth. It denotes the percentage of language queries having at least one segment whose IoU with ground truth is larger than m. In our experiments, we use  $n \in \{1, 5\}$  for all datasets,  $m \in \{0.5, 0.7\}$  for ActivityNet Caption and Charades-STA, and  $m \in \{0.3, 0.5\}$  for TACoS.

## 4.2 Implementation details

Following [24, 53], for video encoding, we apply a pre-trained C3D network [43] to obtain embedded features on all three datasets. Besides, we also extract the I3D [4] and VGG [41] features on Charades-STA for fair comparison with some previous works. After that, we downsample the feature sequence of each video to 200 for ActivityNet Caption and TACoS, and 64 for Charades-STA. For sentence encoding, we utilize the Glove model [35] to embed word-level features. The feature dimension  $D$  is set to 512, and the head in multi-head self-attention is set to 8. The number of predicted positive frames is  $K = 5$ . The hyper-parameters  $\alpha_1, \alpha_2$  in matching score are set to 0.6, 0.4 respectively, and the hyper-parameters  $\gamma_1, \gamma_2$  in matching loss are set to  $\gamma_1 = 1.0, \gamma_2 = 0.5$  respectively. The margin parameters are set to  $\beta_1 = \beta_2 = 0.2$ . To infer the adjacent frames, we set the threshold as  $\Theta = 0.75$  in our all experiments. During the training, we warm up our SL module with an Adam optimizer for 50 epochs, and train the BP module and finetune the whole SLP model for 50 and 100 epochs, respectively. The initial learning rate is set to 0.0001 and it is divided by 10 when the loss arrives on plateaus.

## 4.3 Comparison with State-of-the-Arts

**Compared methods.** We compare the proposed SLP with state-of-the-art NLVL methods on three datasets. These methods are grouped into two categories by the viewpoints of proposal-based and proposal-free approach: (1) Proposal-based approach: CTRL [12], QSPN [47], SCDM [51], CMIN [60], DRN [53], 2DTAN [59], CBLN [24], GTR [3]; These methods first sample multiple candidate video segments, and then directly compute the semantic similarity between the query representations with segment representations for ranking and selection. (2) Proposal-free approach: LGI [33], VSLNet [57], IVG-DCL [34], SeqPAN [56], MATN [58]; These methods directly predict the start and end timestamps of the target

**Table 1: Performance comparison with the state-of-the-art NLVL models on the ActivityNet Caption dataset.**

Method	Feature	R@1, IoU=0.5	R@1, IoU=0.7	R@5, IoU=0.5	R@5, IoU=0.7
CTRL [12]	C3D	29.01	10.34	59.17	37.54
QSPN [47]	C3D	33.26	13.43	62.39	40.78
SCDM [51]	C3D	36.75	19.86	64.99	41.53
LGI [33]	C3D	41.51	23.07	-	-
VSLNet [57]	C3D	43.22	26.16	-	-
IVG-DCL [34]	C3D	43.84	27.10	-	-
CMIN [60]	C3D	43.40	23.88	67.95	50.73
DRN [53]	C3D	45.45	24.36	77.97	50.30
2DTAN [59]	C3D	44.51	26.54	77.13	61.96
SeqPAN [56]	C3D	45.50	28.37	-	-
MATN [58]	C3D	48.02	31.78	78.02	63.18
CBLN [24]	C3D	48.12	27.60	79.32	63.41
GTR [3]	C3D	50.57	29.11	80.43	65.14
<b>SLP</b>	C3D	<b>52.89</b>	<b>32.04</b>	<b>82.65</b>	<b>67.21</b>

**Table 2: Performance comparison with the state-of-the-art NLVL models on the TACoS dataset.**

Method	Feature	R@1, IoU=0.3	R@1, IoU=0.5	R@5, IoU=0.3	R@5, IoU=0.5
CTRL [12]	C3D	18.32	13.30	36.69	25.42
QSPN [47]	C3D	20.15	15.23	36.72	25.30
SCDM [51]	C3D	26.11	21.17	40.16	32.18
VSLNet [57]	C3D	29.61	24.27	-	-
CMIN [60]	C3D	24.64	18.05	38.46	27.02
DRN [53]	C3D	-	23.17	-	33.36
SeqPAN [56]	C3D	31.72	27.19	-	-
2DTAN [59]	C3D	37.29	25.32	57.81	45.04
IVG-DCL [34]	C3D	38.84	29.07	-	-
CBLN [24]	C3D	38.98	27.65	59.96	46.24
GTR [3]	C3D	40.39	30.22	61.94	47.73
<b>SLP</b>	C3D	<b>42.73</b>	<b>32.58</b>	<b>64.30</b>	<b>50.17</b>

segment by regression. In all result tables, the scores of compared methods are reported in the corresponding papers.

**Comparison on ActivityNet Caption.** As shown in Table 1, we compare our SLP with the state-of-the-art proposal-based and proposal-free methods on ActivityNet Caption dataset, where we achieve a new state-of-the-art performance in terms of all metrics. Particularly, the proposed SLP model outperforms the best proposal-based method GTR with 2.32%, 2.93%, 2.22% and 2.07% improvements on the all metrics, respectively. It also makes an even larger improvement over the best proposal-free method MATN in metrics R@1, IoU=0.5 and R@1, IoU=0.5 by 4.87% and 4.63%. It verifies the benefits of utilizing two-step localization framework to predict the fine-grained positive frames and capture the detailed differences among the consecutive frames.

**Comparison on TACoS.** We also compare SLP with the state-of-the-art proposal-based and proposal-free methods on the TACoS dataset in Table 2. On TACoS dataset, the cooking activities take place in the same kitchen scene with slightly varied cooking objects, thus showing the challenging nature of this dataset. Despite



**Table 3: Performance comparison with the state-of-the-art NLVL models on the Charades-STA dataset.**

Method	Feature	R@1, IoU=0.5	R@1, IoU=0.7	R@5, IoU=0.5	R@5, IoU=0.7
2DTAN [59]	VGG	39.81	23.25	79.33	51.15
DRN [53]	VGG	42.90	23.68	87.80	54.87
CBLN [24]	VGG	43.67	24.44	88.39	56.49
<b>SLP</b>	VGG	<b>45.83</b>	<b>26.15</b>	<b>90.52</b>	<b>58.31</b>
CTRL [12]	C3D	23.63	8.89	58.92	29.57
QSPN [47]	C3D	35.60	15.80	79.40	45.40
DRN [53]	C3D	45.40	26.40	88.01	55.38
CBLN [24]	C3D	47.94	28.22	88.20	57.47
<b>SLP</b>	C3D	<b>49.26</b>	<b>30.09</b>	<b>90.14</b>	<b>58.80</b>
DRN [53]	I3D	53.09	31.75	89.06	60.05
SCDM [51]	I3D	54.44	33.43	74.43	58.08
LGI [33]	I3D	59.46	35.48	-	-
CBLN [24]	I3D	61.13	38.22	90.33	61.69
<b>SLP</b>	I3D	<b>64.35</b>	<b>40.43</b>	<b>92.68</b>	<b>63.22</b>

**Table 4: Main ablation studies on the ActivityNet Caption dataset, where ‘MME’ and ‘QCC’ denote the multi-modal encoders and query-guided content comprehension.**

Model	SL Module		BP Module	R@1, IoU=0.5	R@1, IoU=0.7
	MME	QCC			
①	✓	×	×	38.95	19.62
②	✓	✓	×	42.78	23.40
③	✓	×	✓	47.31	27.59
④	✓	✓	✓	<b>52.89</b>	<b>32.04</b>

its difficulty, we still reach the highest results over all evaluation metrics. Particularly, our SLP outperforms the best proposal-based method GTR by 2.36% and 2.44% absolute improvement in terms of R@1, IoU=0.7 and R@5, IoU=0.7, respectively. Compared to the proposal-free method IVG-DCL, it outperforms it by 3.89% and 3.51% in terms of R@1, IoU=0.5 and R@1, IoU=0.7, respectively.

**Comparison on Charades-STA.** Table 3 also report the comparison of localization results on Charades-STA dataset. For fair comparison with different methods, we perform experiments with same features (*i.e.*, VGG, C3D, and I3D) reported in their papers. We can find that our SLP reaches the highest results over all evaluation metrics. Specifically, when using the same VGG features, compared to the previously best method CBLN, our model brings the absolute improvement of 2.16%, 1.71%, 2.13% and 1.82% on all metrics, respectively. When using the same C3D or I3D features, it is obvious that our model still performs better than the existing methods. All these results again verify the effectiveness of our model.

#### 4.4 Ablation Study

In this section, we perform in-depth ablation studies to analyze the effectiveness of our proposed SLP. Specifically, We first conduct the main ablation study to investigate the contribution of each components, then examine the effectiveness of SL and BP modules, and analyze the impact of different settings on hyper-parameters.

**Table 5: Investigation on the Skimming-and-Locating (SL) module on the ActivityNet Caption dataset.**

Components	Variants	R@1, IoU=0.5	R@1, IoU=0.7
MME	w/o transformer	50.27	30.53
	w/ transformer	<b>52.89</b>	<b>32.04</b>
QCC	graph layer=0	48.07	28.82
	graph layer=1	<b>52.89</b>	<b>32.04</b>
	graph layer=2	51.16	30.95

**Table 6: Investigation on the Bi-directional Perusing (BP) module on the ActivityNet Caption dataset.**

Components	Variants	R@1, IoU=0.5	R@1, IoU=0.7
Directional Perusing	left-then-right	<b>53.06</b>	31.81
	right-then-left	52.93	31.97
	left-while-right	52.89	<b>32.04</b>
Segment Update	w/ max-pooling	49.51	28.20
	w/ concatenation	51.66	30.75
	w/ update	<b>52.89</b>	<b>32.04</b>

**Main ablation study.** As shown in Table 4, we verify the contribution of each component in our SLP. For SL module, it consists of a multi-modal encoder (MME) and the query-guided content comprehension module (QCC). We first implement the baseline model ① by directly regressing the start/end timestamps based on the encoded video and query features. In this model, we simply utilize a common co-attention mechanism [30] for multi-modal interaction and adopt the boundary regression head as in [57]. After adding the QCC module in model ②, we find that QCC effectively enhances the discriminative frame-wise representation learning, bringing a large improvement gains of 3.83% and 3.78% in terms of R@1, IoU=0.5 and R@1, IoU=0.7. Here, the model ② can be taken as a variant of a single-step model. By combing the SL module ② with the BP module to model ④, there are the most significant improvement of 10.11% and 8.64% since the BP module captures more fine-grained differences between consecutive frames than the single-step regression head. It demonstrates that our two-step framework is effective to generate more accurate target segments.

**Ablation study on the SL module.** As shown in Table 5, we first investigate the impact on different variants of multi-modal encoders (MME). As the multi-head self-attention in MME is a variant of transformer encoder, we remove it in both video and query encoders for comparison. It shows that w/ transformer brings significant improvement since it captures the long-range dependencies among frames/words. Then, we investigate the impact on different layers of the multi-modal graph in QCC. As shown in Table 5, comparing with the model w/o multi-modal graph (graph layer=0), our full model w/multi-modal graph is effective to enhance the discriminative frame-wise feature learning for better classifying positive-negative frame, and achieves the best result with a single layer. More graph layers will result in over-smoothing [20] problem.

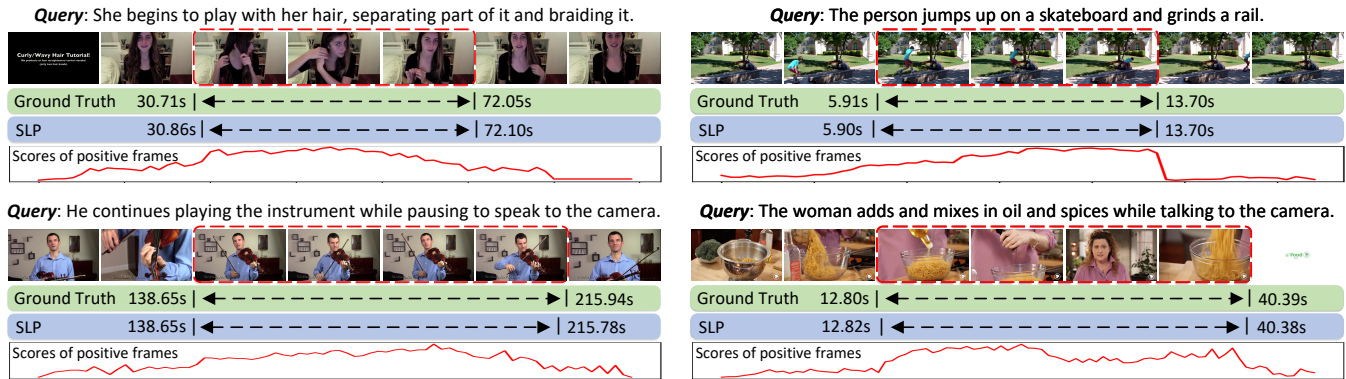


**Figure 3: Qualitative results of our SLP on the ActivityNet Caption dataset. The red curve denotes the frame-wise score obtained by the binary classification function in SL module for predicting the positive frames.**

**Table 7: Sensitivity analysis on the hyper-parameters  $K$ ,  $\alpha_1$ ,  $\alpha_2$  and  $\Theta$  on the ActivityNet Caption dataset.**

Variable	$K$	$\alpha_1$	$\alpha_2$	$\Theta$	R@1, IoU=0.5	R@1, IoU=0.7
$K$	1	0.6	0.4	0.75	49.85	30.14
	3	0.6	0.4	0.75	51.57	31.23
	5	0.6	0.4	0.75	52.89	<b>32.04</b>
	7	0.6	0.4	0.75	<b>52.92</b>	<b>32.04</b>
$\alpha_1, \alpha_2$	5	0.0	1.0	0.75	47.69	27.17
	5	0.2	0.8	0.75	50.06	29.40
	5	0.4	0.6	0.75	51.77	31.23
	5	0.6	0.4	0.75	<b>52.89</b>	<b>32.04</b>
	5	0.8	0.2	0.75	52.35	31.62
$\Theta$	5	0.6	0.4	0.60	48.59	29.02
	5	0.6	0.4	0.65	50.17	30.23
	5	0.6	0.4	0.70	51.44	31.35
	5	0.6	0.4	0.75	<b>52.89</b>	<b>32.04</b>
	5	0.6	0.4	0.80	51.60	31.47
	5	0.6	0.4	0.85	51.01	30.58

**Ablation study on the BP module.** For BP module, we first investigate the impact of different directions of the perusing process: 1) first perusing the left frames until no frame matches the target semantic (“left-then-right”); 2) first perusing the right frames until no frame matches the target semantic (“right-then-left”); 3) perusing the left and right frames at the same time (“left-while-right”). As shown in Table 6, there is no significant difference in the performances of different perusing directions, which indicates our SLP model is insensitive to the directions of perusing. Therefore, we utilize the “left-while-right” perusing direction in all experiments. We also investigate the effectiveness of different strategies for integrating features of new input frame with the current segment. It shows that our learnable selective segment updating strategy performs better than both max-pooling and concatenation operations.

**Impact of hyper-parameters.** We first analyze the impact of different number  $K$  of the predicted top ranked positive frames. As shown in Table 7, a larger  $K$  results in more accurate localization,

leading to precise segment boundary. This is because some false-positive predicted frames degenerate the performance when the number  $K$  is small. The model with  $K = 7$  achieves the best result but only performs marginally better than that with  $K = 5$  at the expense of significantly larger cost of GPU memory and time. Therefore, we choose  $K = 5$  in all the experiments. We then analyze the balancing weights  $\alpha_1, \alpha_2$  of the linguistic and visual similarity scores in Equation (8). Table 7 shows that both scores are crucial to the final matching, where the model with  $\alpha_1 = 0.6, \alpha_2 = 0.4$  achieves the best result. It also shows that the linguistic score is a bit more important than the visual one, since some complicated visual appearances among consecutive frames are harder to distinguish. At last, we evaluate the model with different thresholds  $\Theta$  to investigate its impact on adjacent frame definition (should add into the current segment or not). Specifically, a larger  $\Theta$  denotes a stricter segment construction. From the table, we see that the model with  $\Theta = 0.75$  performs the best. Overall, the performance changes only a small amount as the hyperparameters are changed.

## 4.5 Visualization Results

To qualitatively validate the effectiveness of our SLP, we investigate the localization results of several typical examples as shown in Figure 3. By deploying the “Skimming-Locating-Perusing” human-like localization strategy, our SLP model captures more fine-grained differences between adjacent frames, thus leading to produce precise segment boundaries. Besides, to investigate the positive-negative classification performance of the SL module, we also plot the scores of the video frames predicted by Equation (7) in Figure 3 (red curve). We can find that the frames with highest scores are almost fall into the ground-truth segment, which demonstrates that the SL module is able to locate the positive frames well.

## 5 CONCLUSION

In this paper, we argued that existing NLVL methods follow the unnatural “only look once” framework and overlook two indispensable characteristics: frame-differentiable and boundary-precise. To this end, we propose a human-like framework called Skimming-Locating-Perusing (SLP), which consists of a Skimming-and-Locating (SL) module and a Bi-directional Perusing (BP) module. The SL module first comprehends the query semantic and interacts it with the



video features to distinguish positive and negative frames. Then, the BP module initializes the segment based on each positive frame and dynamically updates it by adding adjacent frames sharing the same semantic. With such "Skimming-Locating-Perusing" localization strategy, we are able to determine more precise segment boundaries. Experimental results on three challenging benchmarks demonstrate the superiority of our SLP compared to the state-of-the-arts.

## REFERENCES

- [1] Lisa Anne Hendricks, Oliver Wang, Eli Shechtman, Josef Sivic, Trevor Darrell, and Bryan Russell. 2017. Localizing moments in video with natural language. In *Proceedings of the IEEE International Conference on Computer Vision (ICCV)*.
- [2] Fabian Caba Heilbron, Victor Escorcia, Bernard Ghanem, and Juan Carlos Nibbles. 2015. Activitynet: A large-scale video benchmark for human activity understanding. In *Proceedings of the IEEE Conference on Computer Vision and Pattern Recognition (CVPR)*.
- [3] Meng Cao, Long Chen, Mike Zheng Shou, Can Zhang, and Yuexian Zou. 2021. On Pursuit of Designing Multi-modal Transformer for Video Grounding. In *Proceedings of the Conference on Empirical Methods in Natural Language Processing (EMNLP)*.
- [4] Joao Carreira and Andrew Zisserman. 2017. Quo vadis, action recognition? a new model and the kinetics dataset. In *Proceedings of the IEEE Conference on Computer Vision and Pattern Recognition (CVPR)*.
- [5] Jingyuan Chen, Xinpeng Chen, Lin Ma, Zequn Jie, and Tat-Seng Chua. 2018. Temporally grounding natural sentence in video. In *Proceedings of the Conference on Empirical Methods in Natural Language Processing (EMNLP)*.
- [6] Kan Chen, Rama Kovvuri, Jiyang Gao, and Ram Nevatia. 2017. MSRC: Multimodal Spatial Regression with Semantic Context for Phrase Grounding. In *Proceedings of the ACM International Conference on Multimedia (ACM MM)*.
- [7] Kan Chen, Rama Kovvuri, and Ram Nevatia. 2017. Query-guided regression network with context policy for phrase grounding. In *Proceedings of the IEEE International Conference on Computer Vision (ICCV)*.
- [8] Long Chen, Chujie Lu, Siliang Tang, Jun Xiao, Dong Zhang, Chile Tan, and Xiaolin Li. 2020. Rethinking the Bottom-Up Framework for Query-based Video Localization. In *Proceedings of the AAAI Conference on Artificial Intelligence*.
- [9] Junyoung Chung, Caglar Gulcehre, KyungHyun Cho, and Yoshua Bengio. 2014. Empirical evaluation of gated recurrent neural networks on sequence modeling. In *Advances in Neural Information Processing Systems (NIPS)*.
- [10] Chaorui Deng, Qi Wu, Qingyao Wu, Fuyuan Hu, Fan Lyu, and Mingkui Tan. 2018. Visual grounding via accumulated attention. In *Proceedings of the IEEE Conference on Computer Vision and Pattern Recognition (CVPR)*.
- [11] Ko Endo, Masaki Aono, Eric Nichols, and Kotaro Funakoshi. 2017. An Attention-based Regression Model for Grounding Textual Phrases in Images. In *IJCAI*.
- [12] Jiyang Gao, Chen Sun, Zhenheng Yang, and Ram Nevatia. 2017. Tall: Temporal activity localization via language query. In *Proceedings of the IEEE International Conference on Computer Vision (ICCV)*.
- [13] Ross Girshick. 2015. Fast r-cnn. In *Proceedings of the IEEE International Conference on Computer Vision (ICCV)*.
- [14] Meera Hahn, Asim Kadav, James M Rehg, and Hans Peter Graf. 2019. Tripping through time: Efficient localization of activities in videos. *arXiv preprint arXiv:1904.09936* (2019).
- [15] Ronghang Hu, Huazhe Xu, Marcus Rohrbach, Jiashi Feng, Kate Saenko, and Trevor Darrell. 2016. Natural language object retrieval. In *Proceedings of the IEEE Conference on Computer Vision and Pattern Recognition (CVPR)*.
- [16] Andrej Karpathy and Li Fei-Fei. 2015. Deep visual-semantic alignments for generating image descriptions. In *Proceedings of the IEEE Conference on Computer Vision and Pattern Recognition (CVPR)*.
- [17] Thomas N Kipf and Max Welling. 2016. Semi-supervised classification with graph convolutional networks. In *Proceedings of the International Conference on Learning Representations (ICLR)*.
- [18] Ranjay Krishna, Kenji Hata, Frederic Ren, Li Fei-Fei, and Juan Carlos Nibbles. 2017. Dense-captioning events in videos. In *Proceedings of the IEEE International Conference on Computer Vision (ICCV)*.
- [19] Huayang Li, Lemaou Liu, Guoping Huang, and Shuming Shi. 2021. GWLAN: General Word-Level AutoCompletion for Computer-Aided Translation. In *Proceedings of the Annual Meeting of the Association for Computational Linguistics (ACL)*.
- [20] Qimai Li, Zhichao Han, and Xiao-Ming Wu. 2018. Deeper insights into graph convolutional networks for semi-supervised learning. In *Proceedings of the AAAI Conference on Artificial Intelligence*.
- [21] Daizong Liu, Xiaoye Qu, Xing Di, Yu Cheng, Zichuan Xu Xu, and Pan Zhou. 2022. Memory-Guided Semantic Learning Network for Temporal Sentence Grounding. In *Proceedings of the AAAI Conference on Artificial Intelligence*.
- [22] Daizong Liu, Xiaoye Qu, Jianfeng Dong, and Pan Zhou. 2020. Reasoning step-by-step: Temporal sentence localization in videos via deep rectification-modulation network. In *Proceedings of the 28th International Conference on Computational Linguistics*.
- [23] Daizong Liu, Xiaoye Qu, Jianfeng Dong, and Pan Zhou. 2021. Adaptive Proposal Generation Network for Temporal Sentence Localization in Videos. In *Proceedings of the 2021 Conference on Empirical Methods in Natural Language Processing (EMNLP)*. 9292–9301.
- [24] Daizong Liu, Xiaoye Qu, Jianfeng Dong, Pan Zhou, Yu Cheng, Wei Wei, Zichuan Xu, and Yulai Xie. 2021. Context-aware Biaffine Localizing Network for Temporal Sentence Grounding. In *Proceedings of the IEEE Conference on Computer Vision and Pattern Recognition (CVPR)*.
- [25] Daizong Liu, Xiaoye Qu, and Wei Hu. 2022. Reducing the Vision and Language Bias for Temporal Sentence Grounding. In *Proceedings of the ACM International Conference on Multimedia (ACM MM)*.
- [26] Daizong Liu, Xiaoye Qu, Xiao-Yang Liu, Jianfeng Dong, Pan Zhou, and Zichuan Xu. 2020. Jointly Cross-and Self-Modal Graph Attention Network for Query-Based Moment Localization. In *Proceedings of the ACM International Conference on Multimedia (ACM MM)*.
- [27] Daizong Liu, Xiaoye Qu, Yinzheng Wang, Xing Di, Kai Zou, Yu Cheng, Zichuan Xu, and Pan Zhou. 2022. Unsupervised Temporal Video Grounding with Deep Semantic Clustering. In *Proceedings of the AAAI Conference on Artificial Intelligence*.
- [28] Daizong Liu, Xiaoye Qu, and Pan Zhou. 2021. Progressively Guide to Attend: An Iterative Alignment Framework for Temporal Sentence Grounding. In *Proceedings of the Conference on Empirical Methods in Natural Language Processing (EMNLP)*.
- [29] Daizong Liu, Xiaoye Qu, Pan Zhou, and Yang Liu. 2022. Exploring Motion and Appearance Information for Temporal Sentence Grounding. In *Proceedings of the AAAI Conference on Artificial Intelligence*.
- [30] Jiasen Lu, Jianwei Yang, Dhruv Batra, and Devi Parikh. 2016. Hierarchical question-image co-attention for visual question answering. In *Advances in Neural Information Processing Systems (NIPS)*.
- [31] Junhua Mao, Jonathan Huang, Alexander Toshev, Oana Camburu, Alan L Yuille, and Kevin Murphy. 2016. Generation and comprehension of unambiguous object descriptions. In *Proceedings of the IEEE Conference on Computer Vision and Pattern Recognition (CVPR)*.
- [32] Yuning Mao, Pengcheng He, Xiaodong Liu, Yelong Shen, Jianfeng Gao, Jiawei Han, and Weizhu Chen. 2021. Generation-augmented retrieval for open-domain question answering. In *Proceedings of the Annual Meeting of the Association for Computational Linguistics (ACL)*.
- [33] Jonghwan Mun, Minsu Cho, and Bohyung Han. 2020. Local-Global Video-Text Interactions for Temporal Grounding. In *Proceedings of the IEEE Conference on Computer Vision and Pattern Recognition (CVPR)*.
- [34] Guoshun Nan, Rui Qiao, Yao Xiao, Jun Liu, Sicong Leng, Hao Zhang, and Wei Lu. 2021. Interventional Video Grounding with Dual Contrastive Learning. In *Proceedings of the IEEE Conference on Computer Vision and Pattern Recognition (CVPR)*.
- [35] Jeffrey Pennington, Richard Socher, and Christopher D Manning. 2014. Glove: Global vectors for word representation. In *Proceedings of the Conference on Empirical Methods in Natural Language Processing (EMNLP)*.
- [36] Michaela Regneri, Marcus Rohrbach, Dominikus Wetzels, Stefan Thater, Bernt Schiele, and Manfred Pinkal. 2013. Grounding action descriptions in videos. *Proceedings of the Annual Meeting of the Association for Computational Linguistics (ACL)* (2013).
- [37] Shaoqing Ren, Kaiming He, Ross Girshick, and Jian Sun. 2015. Faster r-cnn: Towards real-time object detection with region proposal networks. In *Advances in Neural Information Processing Systems (NIPS)*.
- [38] Cristian Rodriguez, Edison Marrese-Taylor, Fatemeh Sadat Saleh, Hongdong Li, and Stephen Gould. 2020. Proposal-free temporal moment localization of a natural-language query in video using guided attention. In *The IEEE Winter Conference on Applications of Computer Vision (WACV)*.
- [39] Anna Rohrbach, Marcus Rohrbach, Ronghang Hu, Trevor Darrell, and Bernt Schiele. 2016. Grounding of textual phrases in images by reconstruction. In *Proceedings of the European Conference on Computer Vision (ECCV)*.
- [40] Gunnar A Sigurdsson, Gül Varol, Xiaolong Wang, Ali Farhadi, Ivan Laptev, and Abhinav Gupta. 2016. Hollywood in homes: Crowdsourcing data collection for activity understanding. In *Proceedings of the European Conference on Computer Vision (ECCV)*.
- [41] Karen Simonyan and Andrew Zisserman. 2014. Very deep convolutional networks for large-scale image recognition. *arXiv preprint arXiv:1409.1556* (2014).
- [42] Joyeeta Singha, Amarjit Roy, and Rabul Hussain Laskar. 2018. Dynamic hand gesture recognition using vision-based approach for human-computer interaction. *Neural Computing and Applications* (2018).
- [43] Du Tran, Lubomir Bourdev, Rob Fergus, Lorenzo Torresani, and Manohar Paluri. 2015. Learning spatiotemporal features with 3d convolutional networks. In *Proceedings of the IEEE International Conference on Computer Vision (ICCV)*.
- [44] Ashish Vaswani, Noam Shazeer, Niki Parmar, Jakob Uszkoreit, Llion Jones, Aidan N Gomez, Łukasz Kaiser, and Illia Polosukhin. 2017. Attention is all you need. In *Advances in Neural Information Processing Systems (NIPS)*.

- [45] Mingzhe Wang, Mahmoud Azab, Noriyuki Kojima, Rada Mihalcea, and Jia Deng. 2016. Structured matching for phrase localization. In *Proceedings of the European Conference on Computer Vision (ECCV)*.
- [46] Jie Wu, Guanbin Li, Si Liu, and Liang Lin. 2020. Tree-structured policy based progressive reinforcement learning for temporally language grounding in video. In *AAAI*, Vol. 34. 12386–12393.
- [47] Huijuan Xu, Kun He, Bryan A Plummer, Leonid Sigal, Stan Sclaroff, and Kate Saenko. 2019. Multilevel language and vision integration for text-to-clip retrieval. In *Proceedings of the AAAI Conference on Artificial Intelligence*.
- [48] Vikas Yadav, Steven Bethard, and Mihai Surdeanu. 2020. Unsupervised alignment-based iterative evidence retrieval for multi-hop question answering. In *Proceedings of the Annual Meeting of the Association for Computational Linguistics (ACL)*.
- [49] Licheng Yu, Zhe Lin, Xiaohui Shen, Jimei Yang, Xin Lu, Mohit Bansal, and Tamara L Berg. 2018. Mattnet: Modular attention network for referring expression comprehension. In *Proceedings of the IEEE Conference on Computer Vision and Pattern Recognition (CVPR)*.
- [50] Licheng Yu, Patrick Poirson, Shan Yang, Alexander C Berg, and Tamara L Berg. 2016. Modeling context in referring expressions. In *Proceedings of the European Conference on Computer Vision (ECCV)*.
- [51] Yitian Yuan, Lin Ma, Jingwen Wang, Wei Liu, and Wenwu Zhu. 2019. Semantic Conditioned Dynamic Modulation for Temporal Sentence Grounding in Videos. In *Advances in Neural Information Processing Systems (NIPS)*.
- [52] Yitian Yuan, Tao Mei, and Wenwu Zhu. 2019. To find where you talk: Temporal sentence localization in video with attention based location regression. In *Proceedings of the AAAI Conference on Artificial Intelligence*.
- [53] Runhao Zeng, Haoming Xu, Wenbing Huang, Peihao Chen, Mingkui Tan, and Chuang Gan. 2020. Dense regression network for video grounding. In *Proceedings of the IEEE Conference on Computer Vision and Pattern Recognition (CVPR)*.
- [54] Da Zhang, Xiyang Dai, Xin Wang, Yuan-Fang Wang, and Larry S Davis. 2019. Man: Moment alignment network for natural language moment retrieval via iterative graph adjustment. In *Proceedings of the IEEE Conference on Computer Vision and Pattern Recognition (CVPR)*.
- [55] Hanwang Zhang, Yulei Niu, and Shih-Fu Chang. 2018. Grounding referring expressions in images by variational context. In *Proceedings of the IEEE Conference on Computer Vision and Pattern Recognition (CVPR)*.
- [56] Hao Zhang, Aixin Sun, Wei Jing, Liangli Zhen, Joey Tianyi Zhou, and Rick Siow Mong Goh. 2021. Parallel Attention Network with Sequence Matching for Video Grounding. *arXiv preprint arXiv:2105.08481* (2021).
- [57] Hao Zhang, Aixin Sun, Wei Jing, and Joey Tianyi Zhou. 2020. Span-based Localizing Network for Natural Language Video Localization. In *Proceedings of the Annual Meeting of the Association for Computational Linguistics (ACL)*.
- [58] Mingxing Zhang, Yang Yang, Xinghan Chen, Yanli Ji, Xing Xu, Jingjing Li, and Heng Tao Shen. 2021. Multi-Stage Aggregated Transformer Network for Temporal Language Localization in Videos. In *Proceedings of the IEEE Conference on Computer Vision and Pattern Recognition (CVPR)*.
- [59] Songyang Zhang, Houwen Peng, Jianlong Fu, and Jiebo Luo. 2020. Learning 2D Temporal Adjacent Networks for Moment Localization with Natural Language. In *Proceedings of the AAAI Conference on Artificial Intelligence*.
- [60] Zhu Zhang, Zhijie Lin, Zhou Zhao, and Zhenxin Xiao. 2019. Cross-modal interaction networks for query-based moment retrieval in videos. In *Proceedings of the 42nd International ACM SIGIR Conference on Research and Development in Information Retrieval (SIGIR)*.